Proceedings of the Institution of Civil Engineers
Structures and Buildings 162
August 2009 Issue SB4
Pages 263–273
doi: 10.1680/stbu.2009.162.4.263

Paper 800098
Received 28/11/2008
Accepted 30/04/2009

Keywords: cables & tendons/ coastal engineering/concrete structures

Paul Scott
PhD candidate, Department of Engineering, University of Cambridge, UK

Janet M. Lees
Senior Lecturer, Department of Engineering, University of Cambridge, UK

ice
Institution of Civil Engineers

Uptake swelling and thermal expansion of CFRP tendons

P. Scott MEng and J. M. Lees PhD

Carbon-fibre-reinforced polymer (CFRP) tendons can be used as a corrosion-resistant alternative to steel for reinforcing or prestressing concrete in aggressive marine environments. The design lives of many civil marine structures often span decades and so the long-term durability of the internal reinforcement is important. One significant, yet overlooked, aspect of CFRP tendon durability is its susceptibility to swell on absorption of aqueous solutions including water and salt water. This paper reviews uptake-induced swelling in CFRP materials and draws comparisons with studies of swelling caused by thermal effects. The diffusion of aqueous solutions and their interaction with the polymer matrix are identified as the primary mechanisms responsible for the swelling. Experimental details are presented that correlate the uptake of water and salt water to swelling observed in CFRP tendons. The results are contrasted with both uptake- and thermal-driven behaviour cited in the literature. Lamé's equations are used to estimate the magnitude of the resulting stresses induced in the surrounding concrete. The practical significance of the findings is discussed, including the potential for cracking in the surrounding concrete cover and the implications for the tendon–concrete bond.

1. INTRODUCTION

The use of advanced composites as internal reinforcement in reinforced or prestressed concrete construction offers a number of advantages. In particular, the long-term durability of fibre-reinforced polymer (FRP) materials holds great promise in the context of life-cycle costing and for use in aggressive environments where the exposure conditions exacerbate the potential for steel corrosion. Examples of such environments include bridge decks and marine environments.

Regardless of the material used internally to reinforce concrete, the possible implications of dimensional changes need to be carefully considered. A relative expansion of the internal reinforcement may lead to cracking or spalling, whereas a relative contraction could lead to bond deterioration. Dimensional changes may result from a number of sources. For example, thermal expansion has been the subject of great interest and indeed it is argued that early Roman attempts to reinforce concrete with bronze failed owing to differences in the thermal expansion coefficients of the two materials, which led to spalling.[1] In contrast, steel and concrete have similar coefficients of thermal expansion. However, the dimensional changes in steel due to the formation of corrosion products can lead to concrete cracking.

This work will review two possible sources of dimensional change in FRP-reinforced or prestressed concrete structures: temperature changes and aqueous solution uptake. Whereas there have been a number of studies to investigate the effect of temperature on FRP-reinforced concrete, the influence of uptake on FRP tendons appears to be less well documented. Experiments were therefore conducted to assess the swelling resulting from the exposure of carbon-fibre-reinforced polymer (CFRP) tendons to water and salt water. These results were then incorporated into a preliminary comparison of the time-dependent swelling effects and the relative magnitude of these effects when compared with dimensional changes owing to temperature. An understanding of these load cases is important because they may dictate aspects such as the minimum required concrete cover and the long-term bond performance.

2. DIMENSIONAL CHANGES IN CFRP TENDONS

FRP reinforcement consists of continuous unidirectional fibres—such as glass, aramid or carbon fibres—in a resin matrix—such as vinylester, polyester or epoxy. In FRP reinforcement, dimensional changes owing to solution uptake or thermal effects are generally dominated by the properties of the matrix. As the fibres act to restrain any expansion or contraction, the dimensional changes in a composite are typically smaller than those in a neat resin exposed to similar conditions. This restraint also means that, owing to the orthotropic nature of uni-directional FRP reinforcement, the expansion parallel to the fibre direction will differ to that in the transverse direction. In the following, the influence of solution uptake and temperature on carbon/epoxy FRP systems is reviewed.

2.1. Solution uptake

In a neat epoxy, swelling occurs due to the opening up of the polymer physical structure as a result of the formation of hydrogen bonds between the dipoles on water molecules and groups on the polymer chains such as hydroxyls (OH groups).[2] This behaviour also causes what is known as plasticisation, a softening effect, which can reduce the shear strength of the polymer. Carbon fibres are generally considered to be impermeable in comparison to the matrix.[3]

In CFRP tendons, studies have found the restraining effect of the fibres to result in either zero[4,5] or negligible[6] swelling parallel to the fibre direction compared with the transverse direction. As a result, this investigation will focus on swelling effects transverse to the fibre direction. Uptake-induced swelling is generally quantified in terms of an increase in strain which reflects an increase in linear dimensions, for example in a laminate, or an increase in diameter and circumference, for example in an FRP tendon. As there were relatively few studies on the uptake-induced swelling of carbon/epoxy composite tendons, relevant experimental investigations into carbon/epoxy laminates were used to form the basis of current knowledge and are summarised in Table 1. One study on epoxy-based glass FRP laminates (Tsai *et al.*[5]) was also included since the matrix material and the salt water and water exposure conditions were relevant to the current work.

The results in Table 1 indicate that the largest swelling strains were generally experienced in the most aggressive environments. But it is necessary to differentiate between swelling that could be expected in practice, and swelling exacerbated by elevated temperatures in accelerated tests, which do not occur under normal service conditions. With the exception of the very large strains measured by Adams and Singh, which were attributed to the blistering of the epoxy and fibre-matrix breakdown,[4] the reported transverse strains are in the region of 0·27 to 1·58%. In a number of studies, these dimensional changes, $\boldsymbol{\varepsilon}_t$, have been correlated with the increase in mass owing to solution uptake, M_t. The relationship between uptake and swelling has been found to be being either linear, linear after an initial period where swelling lags behind the uptake[11] or slightly accelerating with time.[7] For linear or near-linear behaviour, $\boldsymbol{\varepsilon}_t(\%)/M_t(\%)$ has been found to range between 0·24 and 0·51.

2.2. Thermal effects

Thermal expansion of materials occurs as absorbed heat increases their internal energy, and causes an increase in inter-atom bond lengths. In FRP tendons, the thermal characteristics are dependent on the type of fibre, type of matrix, volume fraction and transverse modulus of elasticity.[12] The coefficients of thermal expansion (CTEs) of two different polyacrylonitrile (PAN)-based carbon fibres have been reported as 3·8 and 5·6 με/°C.[13] These values are typically much smaller than those of matrix materials and so are often considered to be insignificant.[7]

The longitudinal CTE of carbon-epoxy composites is regularly cited as being negative[14,15] or zero but again is generally considered negligible in comparison with the transverse CTE.[12,15–18] For this reason, and to allow parallels to be drawn with uptake-induced swelling, only transverse thermal expansion will be considered. The transverse CTE may exhibit temperature dependency,[7,8,11,19] particularly when exposure temperatures cross the glass transition temperature.[20] However, the variation is sufficiently small over typical in-service conditions for civil engineering structures that an average value is often assumed.[12,15,19,20] A literature survey of experimentally obtained values of transverse CTE for various unidirectional carbon fibre/epoxy products covering fibre volume fractions ranging from 0·58 to 0·65 suggest values between 25 and 47 με/°C.[8,14,15,19,21,22] Regarding guidelines for designers, the ACI Committee 440[23] quotes an envelope encompassing 74·0 to 104·0 με/°C as suitable values of transverse CTE for use when designing with CFRP. These values appear to be higher than those observed experimentally but may represent conservative values for design.

2.3 Implications of dimensional changes in FRP/concrete systems

While both solution uptake and heating may cause internal damage and/or changes in the properties of the FRP itself, a further consideration in reinforced or prestressed concrete applications is the interaction with the concrete. Any relative expansion of an FRP rod in concrete will induce tensile stresses in the surrounding concrete, which may lead to cracking and, in extreme cases, splitting. Furthermore, changes at the tendon–concrete interface either due to local cracking or changes in contact stress will have potential implications on the bond.

While the possibility of uptake-induced splitting exists, no such reports have been found in the literature. However, numerous studies cite the risk of concrete cracking due to tensile stresses induced by thermal expansion of FRP tendons,[17,18,22,24–26] while the risk of tendons separating from the concrete due to contraction is also noted.[17] Nanni *et al.*[24] report thermal expansion of FRP prestressing tendons causing splitting of concrete parallel to FRP tendons within one year of service. A number of studies have demonstrated experimentally the occurrence of concrete cracking owing to thermal expansion of FRP tendons.[12,25–27] An example of such a study is that by Aiello *et al.*[28] who showed that a temperature change of 30°C in a GFRP bar (13 mm diameter, $\alpha_{ft} = 58$ με/°C) encased in a 19 mm thick concrete tube ($\alpha_c = 12$ με/°C, 3·9 MPa tensile strength) was sufficient to cause cracking. The possibility of concrete splitting and how such effects could be modelled are explored in later sections.

3. EXPERIMENTAL INVESTIGATION OF UPTAKE-INDUCED SWELLING IN CFRP TENDONS

In order to expand the experimental database relating to the swelling characteristics of composites and to characterise the solution uptake behaviour of the cylindrical CFRP tendons studied in the current work, experiments were carried out to measure the percentage mass increase and the diameter change of the tendons when exposed to solution. Both water and salt water solutions were considered to investigate the effect of aqueous solution type on swelling.

3.1. Specimen preparation

The key properties of the CFRP tendons studied are shown in Table 2. One complication from an experimental point of view was that the tendons were supplied with a sand coating (used to increase the bond between the concrete and the tendon). This had to be removed as there was no obvious way to take repeatable diameter measurements with the sand coating intact.

Three methods to remove the coating were investigated: manual removal, machining and cylindrical grinding. It was found that cylindrical grinding gave the most repeatable diameter readings and so was used for the preparation of the specimens described in the current work. The cylindrical

Author(s)	Materials* [*f*] = fibre [*m*] = matrix (manufacturer)	Thickness: mm	Exposure time: days	Exposure temp.: °C	Exposure environment	Strain transverse to fibre direction: %	Saturation achieved by end of test	Relationship to uptake	ε_t: %/M_t: %
Cairns and Adams[7]	AS/3501-6 (Hercules)	No data	30	65·5	98% RH	0·83	No	c	—
Adams and Singh[4]	913 (Ciba-Geigy): [*m*] TS carbon: [*f*]	2·0	58	100	Steam	5·92	No	No data	—
	914 (Ciba-Geigy): [*m*] XAS carbon: [*f*]		58			1·00	Yes	—	—
Abot *et al.*[6]	AGP370-5H: [*m*] 3501-6S: [*f*]	2·5	140	55	Distilled water	1·02	No	b	0·24–0·27
Collings and Stone[8]	914 (Ciba-Geigy): [*m*] XAS carbon: [*f*]	0·5	No data	60	59% RH 75% RH 90% RH	0·27 0·37 0·43	Yes	a	0·30 0·31 0·25
Tsai *et al.*[9]	ACD8801: [*m*] HTA1200A: [*f*]	0·57	30	60	90% RH	1·70	Yes	No data	—
Tsai *et al.*[5]	FR-4 (novolac) E-glass: [*f*] **	0·05	28	25	Water 5% wt sodium chloride 10% wt sodium chloride	1·36 1·52 1·58	No	a	—
Wright[10]	5209 (Narmco): [*m*] T300: [*f*]	No data	No data	No data	No data	0·71	No data	a	0·51

** Glass FRP
a Linear
b Initial acceleration of swelling as uptake proceeds, followed by linear behaviour
c Subtle non-linearity: swelling accelerates as uptake proceeds

Table 1. Observed swelling of epoxy matrix composites due to solution uptake

Fibres	Carbon (PAN) [Tenax UTS 5131]
Matrix	Epoxy resin [Rütapox EPR 04434]
Fibre volume fraction: V_f	0·63
Tendon diameter: d	4·2 mm
Coefficient of thermal expansion: α_{ft}*	32·5 $\pm$ 2·5 με/°C

* Manufacturer data supplied by SACAC

Table 2. Properties of CFRP tendons studied

grinding was carried out on a lathe rotating at 6600 rpm with a $\frac{1}{2}$ inch diameter Norton 32A60-KVBE grinding wheel rotating at 200 rpm in the same direction. One concern was whether the removal of the sand coating would inadvertently influence the swelling measurements. Therefore scanning electron microscope (SEM) images of the cylindrically ground specimen surfaces prior to exposure were taken as shown in Figure 1. Although the surface profiles exhibited an inevitable degree of variability, these appeared to be superficial, and were not thought to affect the bulk behaviour in the longer term.

3.2. Experimental procedure for diameter readings

To ensure the repeatability of the diameter measurements, modifications were made to the standard 100 nm resolution universal horizontal metroscope set-up shown in Figure 2. Two sleeves were manufactured to fit over the metroscope jaws as shown in Figure 3 and steel ball-bearing seats were used to centre the sleeves on the jaws at a point. The end profile of one sleeve was flat, and the other was 'V' shaped. By making these features only 1 mm thick, the tendon contact region was localised. Furthermore, the three points of contact between the sleeves and the tendon ensured a fixed angle between the bodies such that a diameter reading could be inferred from the measured distance between the sleeve faces (see Figure 3).

Alignment markers on the sleeves and the tendons were used to ensure that the diameter readings on the tendons were taken at the same position each time. In addition, the measurement system was calibrated using a highly cylindrical steel pin of known diameter before each set of readings. To assess the accuracy and repeatability of the sleeve system, ten diameter readings of a cylindrically ground tendon at a marked location were taken. The mean and standard deviation were found to be 3·9390 mm and 0·0004 mm respectively, which suggests the measurement technique is repeatable.

3.3. Specimen exposure and results

In preparation for the exposure tests, ten specimens were cylindrically ground, then cut to 80 mm lengths. Initial diameter and mass readings of the dry specimens were taken prior to exposure. The exposure conditions reported here were deionised water (W) and salt water (SW), which consisted of 3·5% by weight sodium chloride (NaCl) dissolved in deionised water. All solutions and specimens were maintained at 20°C for the duration of the experiments. To take a reading, the tendons were removed from solution and rinsed in deionised water. They were then blotted dry.

3.3.1. Mass uptake. Mass uptake readings were taken on the same tendons immediately prior to taking diameter measurements. A Mettler AE160 balance of 0·1 mg resolution was used to measure change in mass and values of percentage mass increase were calculated. Figure 4 shows the mean values of each set of readings, where each data point represents the average of the readings for five specimens. Error bars indicating $\pm$ 2 standard deviations are also noted. This figure indicates typical diffusion behaviour with the percentage mass increase initially rising proportionally to the square root of time. The nature of the aqueous solution makes little difference to the uptake, with water exposure giving a slightly higher uptake than salt water exposure. Low data scatter gives confidence in the measurement technique.

3.3.2. Diameter change. Using the method described previously, six diameter readings were then taken on each of the tendon samples—two repetitions at each of three 120° rotation intervals. The transverse strain readings were calculated by dividing the increase in the tendon radius, Δr, by the initial radius r_0.

The average results, based on the readings from five specimens, from the swelling measurements are shown in Figure 5 with error bars indicating $\pm$ 2 standard deviations about the mean. It can be seen in Figure 5 that the mean % increase in transverse strain after 565 days (approximately 1·6 years) was around 0·16% and 0·12% for water and salt water exposure respectively. These results are at the lower end of the ranges reported in Table 1, although it is important to note that saturation had not yet occurred.

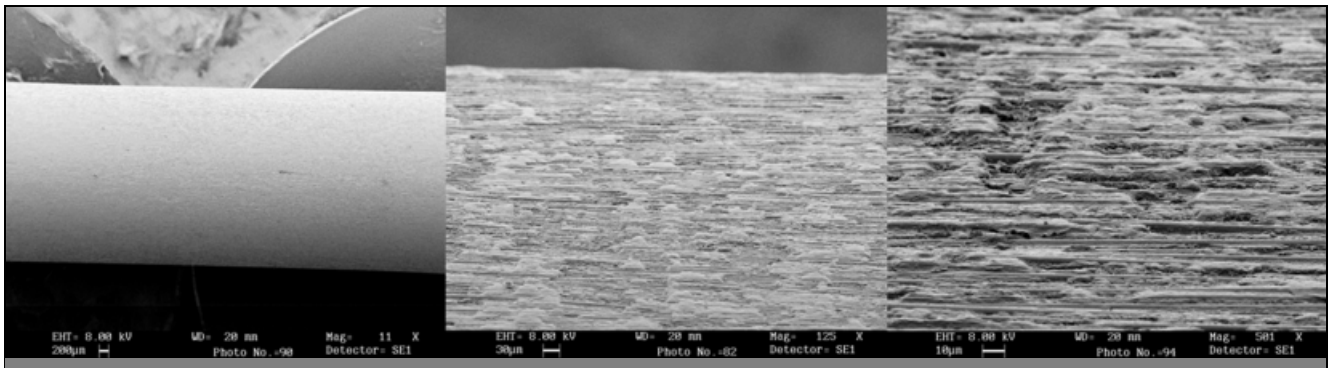

Figure 1. SEM images of cylindrically ground tendon surface

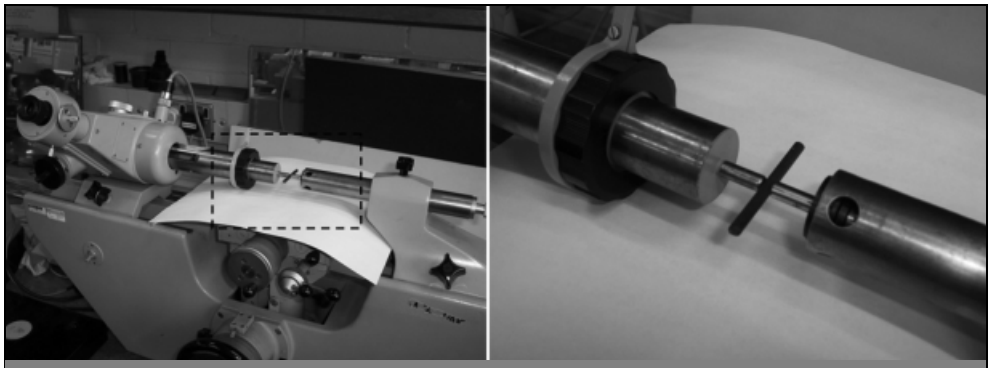

Figure 2. Diameter measurement taken using a universal horizontal metroscope without sleeves

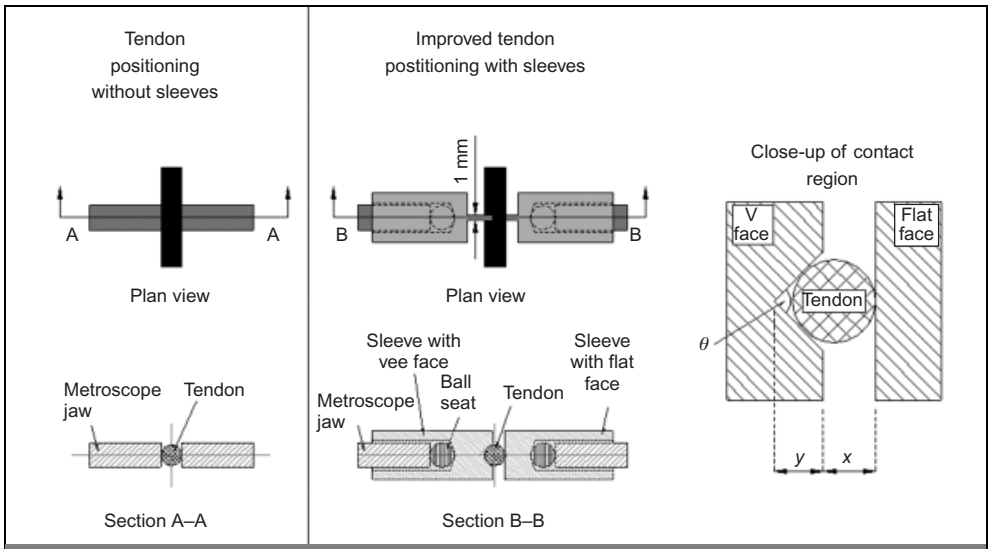

Figure 3. Schematic of sleeves used to improve tendon positioning

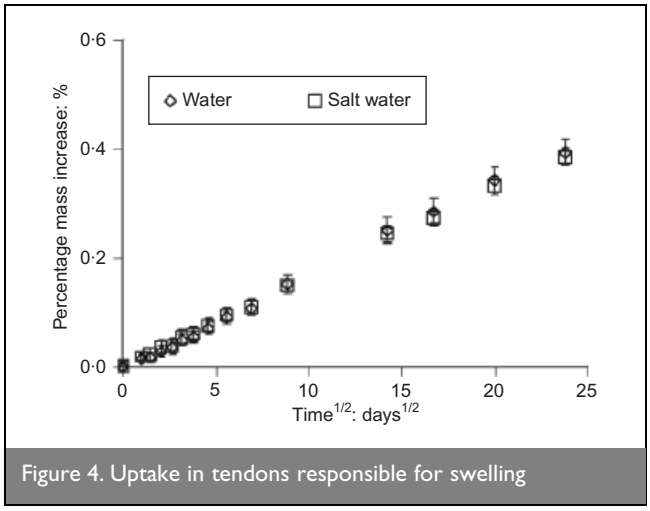

Figure 4. Uptake in tendons responsible for swelling

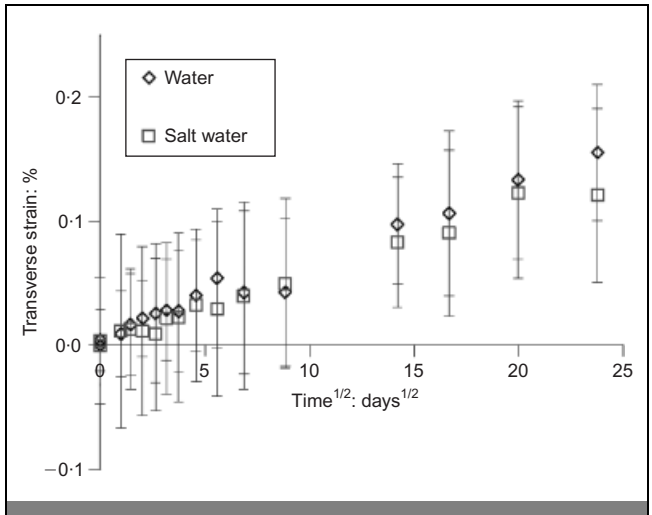

Figure 5. Transverse strain in CFRP tendons as a result of uptake-induced swelling

In Figure 6(a) the transverse strain results are plotted against the mass uptake measurements. Within the measured timeframe, there appears to be a fairly linear relationship between these two quantities. By curve-fitting a linear relationship to the experimental results, the following best-fit expressions were obtained

1	(W)	$\varepsilon_t = 0{\cdot}363 M_t + 0{\cdot}0073$
2	(SW)	$\varepsilon_t = 0{\cdot}329 M_t + 0{\cdot}0023$

where M_t is represented as a percentage. The coefficients, 0·363 and 0·329, and the linear nature of the relationship between uptake and swelling are consistent with findings reported in the literature (see Table 1). As both the water and salt water

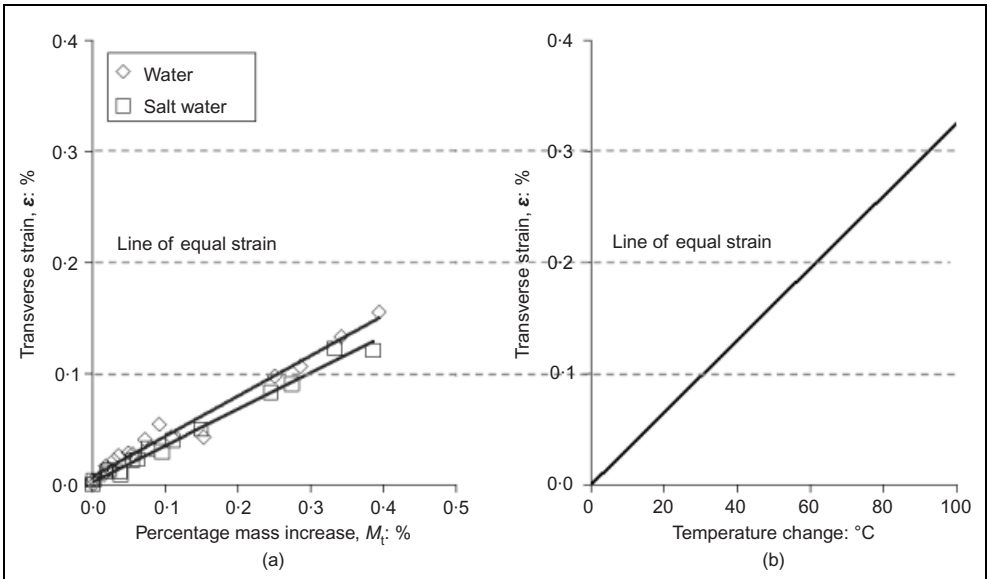

Figure 6. (a) Relationship between solution uptake and swelling in CFRP tendons; (b) predicted expansion owing to a temperature change

uptake appear to be fairly similar, the results also suggest that it is the quantity of solution absorbed into the tendons, rather than the specific nature of the aqueous solution used, that determines the swelling observed. This implies that aqueous solutions to which CFRP tendons may be exposed interact with the polymer chains of an epoxy in much the same way.

3.4. Comparison with thermal strains

To compare solution uptake and temperature effects in a tendon in isolation, the predicted transverse strain increase over a range of temperature changes has been plotted in Figure 6(b). For these thermal calculations, a CTE of 32·5 με/°C (based on the manufacturer's values in Table 2) was assumed. Lines of equal strain are indicated.

Despite the assumption that uptake-induced swelling in a material is temperature-independent, Figure 6 shows strains caused by uptake-induced swelling may exceed strains caused by thermal expansion effects. Furthermore, the tendons studied had not reached saturation, so even greater swelling strains could be expected in practice. Although the magnitudes of uptake-induced swelling may exceed thermal expansion effects, it is important to note that it will occur at a much slower rate, given the rapid nature of heat diffusion through composite materials. On a material level, this means that over sustained periods of time, dimensional changes due to swelling are likely to be significantly more non-uniform in an FRP cross-section than those arising as a result of thermal effects. One negative effect of this is that the regions of the tendon furthest from the centre will initially swell more than regions closer to the centre, reducing the curing-induced compressive stress in the matrix between these regions. This introduces the possibility of a reduced fibre–matrix bond strength or even microcracking.[29]

4. STRESSES GENERATED IN CONCRETE DUE TO SWELLING AND THERMAL EFFECTS

In a concrete reinforcing application, the slower rate of uptake-induced swelling will allow the concrete time to creep. It is therefore of interest to compare estimations of concrete stresses owing to progressive uptake-induced swelling and immediate thermal expansion of an FRP tendon. The particular focus in the current work is the conditions at first cracking. However, the role of the concrete cover in the post-cracking stages will also be discussed in the context of the implications of uptake-induced swelling on the design of reinforced or prestressed concrete structures.

4.1. First cracking: thick-walled cylinder analysis

To predict the elastic stress distribution in concrete subjected to an internal radial pressure, it is common to use a thick-walled cylinder analogy based on Lamé's equations.[30] The hoop stresses, $\boldsymbol{\sigma}_{\theta,2}$, and radial stresses, $\boldsymbol{\sigma}_{r,2}$, induced in the surrounding concrete by an expansive strain, $\boldsymbol{\varepsilon}$, in a tendon can be estimated as a function of radial position, r, using Lamé's equations for thick-walled cylinders. The concrete has a Young's modulus E_c and Poisson's ratio ν_c, whereas the FRP tendon has a transverse Young's modulus E_{22} and transverse Poisson's ratio ν_{23}. It is assumed that the axial stress, $\boldsymbol{\sigma}_z$, in both bodies is zero at all points.

Figure 7 shows a tendon (body 1), of radius r_t, encased by a ring of concrete (body 2) of thickness, c, analogous to the cover. Shown adjacent to the cross-section is a section indicating the interference between the bodies that will occur when the unrestrained tendon radius increases by an amount, i. This expansion creates a radial pressure across the interface, $\boldsymbol{p}$, which causes the inner radius of the concrete shell to displace outwards by an amount i_2, and the outer radius of the tendon to displace inwards by an amount i_1, the sum of which equals i. By using equilibrium, compatibility and the relevant material laws, expressions for the radial pressure at the interface and the hoop and radial stresses in the concrete can be developed in terms of the expansive strain $\boldsymbol{\varepsilon}_r$, where

$$\boldsymbol{p} = \frac{\boldsymbol{\varepsilon}_r E_{22} E_c (c^2 + 2 r_t c)}{(1 - \nu_{23}) E_c c (c + 2 r_t) + E_{22} r_t^2 (1 - \nu_c) + E_{22} (r_t + c)^2 (1 + \upsilon_c)} \quad (3)$$

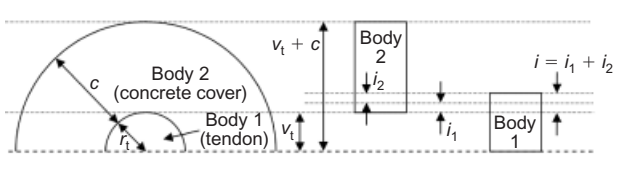

Figure 7. Schematic of tendon swelling encased by ring of concrete

$$4 \quad \sigma_{\theta,2} = \frac{\varepsilon_r E_{22} E_c (2r_t^2 + 2r_t c + c^2)}{E_c c(1-\nu_{23})(c+2r_t) + E_{22} r_t^2 (1-\nu_c) + E_{22}(r_t + c)^2 (1+\upsilon_c)}$$

$$5 \quad \sigma_{r,2} = \frac{-\varepsilon_r E_{22} E_c (2r_t c + c^2)}{E_c c(1-\nu_{23})(c+2r_t) + E_{22} r_t^2 (1-\nu_c) + E_{22}(r_t + c)^2 (1+\upsilon_c)}$$

From Equations 4 and 5, it can be seen that the hoop stress will exceed the radial stress, and that these stresses will be greatest at the interface between the tendon and the concrete. Therefore, these equations can be used to identify when first cracking occurs, namely when the hoop stress reaches the tensile strength of the concrete.

For thermal effects, an effective radial strain, $\varepsilon_{eff,T}$, is used as ε_r, where the expansion of the concrete with a CTE of α_c is subtracted from the expansion of the FRP tendon[12]

$$6 \quad \varepsilon_{eff,T} = (\alpha_{ft} - \alpha_c)\Delta T$$

In wet conditions, swelling strains will increase with time and, as shown in the current work and elsewhere, the radial uptake-induced swelling strain can be taken as roughly proportional to the uptake. For the concrete, Neville[31] has described uptake-induced strains of up to 0·015% in concrete which, relative to the expected expansion of the tendon, can be considered negligible. Hence Equation 7 can be proposed to relate effective swelling strain, $\varepsilon_{eff,M}$, to a quantity of solution uptake characterised by a change in percentage mass increase, ΔM, using a coefficient, β_{ft}

$$7 \quad \varepsilon_{eff,M} = \beta_{ft} \Delta M$$

where β_{ft} reflects the type of solution and relates the mass uptake to radial strain (e.g. Equations 1 and 2). To model the stresses due to swelling at a given time t, $\varepsilon_{eff,M}$, is used as ε_r.

4.2 Time-dependent effects: concrete creep

The timeframe over which thermal and solution uptake effects occur will potentially differ. Whereas swelling is expected to be a gradual process, thermal changes can occur fairly rapidly. As a result, an initial study of time-dependent effects is required to enable comparison of the relative dimensional changes. This time-dependency has analogies to work reported elsewhere, for example Liu and Weyers[32] in the context of steel corrosion.

To account for the concrete creep that will occur over time, the concrete can be assigned an age-adjusted effective modulus (AAEM), $\bar{E}_e$ (Gilbert and Mickleborough[33]) where

$$8 \quad \bar{E}_e = \frac{E_c}{1 + \chi(t, \tau)\phi(t, \tau)}$$

and $\bar{E}_e$ depends on the nominal initial concrete modulus, E_c, an ageing coefficient $\chi(t, \tau)$ and a creep coefficient $\phi(t, \tau)$. These coefficients are functions of the time after casting at which loading commenced, τ, and the time, t, at which $\bar{E}_e$ is calculated.

The ageing coefficient is taken for most practical purposes to be 0·8, although more accurate, yet complex, estimates have been made.[33] The creep coefficient is the ratio of creep strain at time t to the instantaneous strain when a constant sustained stress is first applied at time τ. The calculation of creep strain has been undertaken by numerous organisations, but one of the more well-known and widely used methods was proposed by ACI Committee 209 (1978). For further details see Gilbert and Mickleborough.[33] In Table 3 the details of the creep coefficient expression and the parameters used in the current work are indicated. These parameters were chosen as being representative of a generic slender high-strength concrete structure with a fairly high volume to surface ratio. Reference was made to Neville[31] when selecting the appropriate air content and aggregate ratio parameters. The concrete was assumed to have a low slump and the exposure conditions were taken to be 80% relative humidity (humid conditions).

Assuming an initial concrete modulus of 35 GPa, Figure 8(a) shows how the creep coefficient can be expected to vary over a 2-year period. The associated AAEM calculated using Equation 8 is shown in Figure 8(b).

These results give an indication of how the concrete stiffness will change with time. The AAEM is stress-independent and the behaviour in tension and compression can also be assumed to be identical.[33] As such, the E_c in Equations 4 and 5 can be replaced with E_{ct}, where E_{ct} is the time-dependent modulus as shown in Figure 8(b). Hence if the tendon properties and the swelling characteristics are known, these expressions can be used to find the associated concrete stress at a given time.

Principal equation	
$\phi(t, \tau) = \frac{(t-\tau)^{0.6}}{10 + (t-\tau)^{0.6}} \phi^*(t)$	
Correction factors	
$\phi^*(t) = 2{\cdot}35\gamma_1\gamma_2\gamma_3\gamma_4\gamma_5\gamma_6$	
$\gamma_1 = 1{\cdot}25\tau^{-0{\cdot}118}$	
$\gamma_2 = 1{\cdot}27 - 0{\cdot}0067(RH)$	
$\gamma_3 = 1{\cdot}3$	
$\gamma_4 = 0{\cdot}82 + 0{\cdot}00264s$	
$\gamma_5 = 0{\cdot}88 + 0{\cdot}0024\psi$	
$\gamma_6 = 0{\cdot}46 + 0{\cdot}09a$	
Parameters	
Slump (s): mm	0
τ: days	5
RH: %	80
Volume/surface ratio: mm	12·5
Fine/course aggregate ratio (ψ): %	50
Air content (a): %	5

Table 3. Calculation of creep coefficient using ACI Committee 209 method

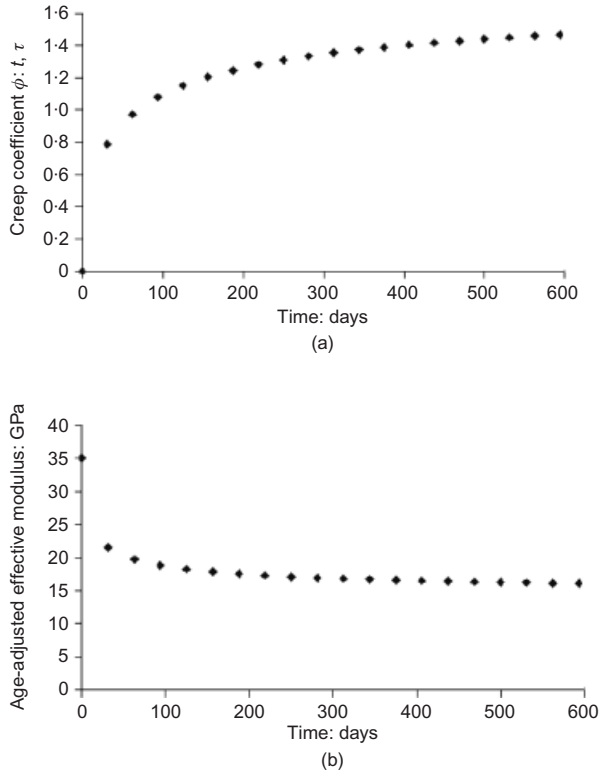

Figure 8. (a) Variation of creep coefficient with respect to time; (b) variation of AAEM with respect to time

4.3. Partially cracked and splitting behaviour

The analysis presented in the previous sections considers the stresses up to first cracking. Once cracking occurs the cylinder can be considered to consist of both cracked and uncracked regions (see Figure 9(a)), a stage which Tepfers[34] describes as the partly cracked elastic stage. Models to predict the partly cracked behaviour have been developed to investigate thermal expansion effects in FRPs in concrete, for example Aiello *et al.*[28] and also the corrosion of internal steel reinforcement, for example Li *et al.*[35] Corrosion cracking models generally incorporate time-dependent concrete effects so could potentially be adapted to reflect FRP swelling. At the limit of the partly cracked stage, a longitudinal crack extends throughout the concrete cover. However, if the concrete deforms plastically, a higher ultimate load may be achieved. Hence, Tepfers[34] also introduces an uncracked plastic stage where the concrete behaves plastically and failure occurs when the stresses throughout the cylinder reach the ultimate tensile stress in the concrete $\boldsymbol{f}_{ct}$ (see Figure 9(b)). This would represent

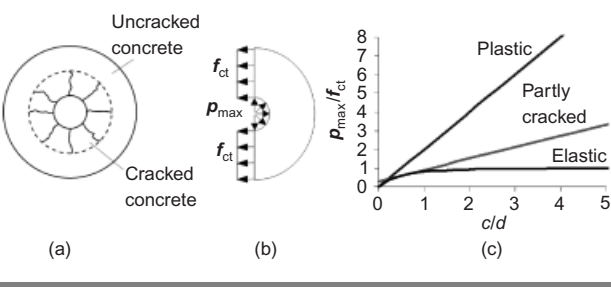

Figure 9. (a) Partly cracked behaviour, (b) plastic behaviour and (c) relationship between $\boldsymbol{p}_{max}/\boldsymbol{f}_{ct}$ and c/d (after Tepfers[34])

an upper bound on the splitting capacity. Tepfers' expressions for the elastic, partly cracked and plastic stages are shown schematically in Figure 9(c) where the ratio of the maximum internal pressure $\boldsymbol{p}_{max}$ divided by the concrete tensile strength $\boldsymbol{f}_{ct}$ has been plotted against the concrete cover over bar diameter ratio (c/d). This figure demonstrates that whereas an increase in concrete cover has a relatively small influence on $\boldsymbol{p}_{max}/\boldsymbol{f}_{ct}$ at first cracking, it does play a significant role in determining when the cracks will propagate to the concrete surface.

4.4. Stress and failure predictions

Predictions were made of the swelling and solution uptake-induced stresses generated between a CFRP tendon equivalent to that used in the experimental programme and a generic high-strength concrete. An elastic thick-walled analysis (Equations 4 and 5) was used with the relevant input parameters as detailed below.

Water exposure was assumed so β_{ft} was taken as 0·363 (Equation 1). The change in ΔM with time is as shown in Figure 4. The CTE of the concrete was taken to be $\alpha_c = 9$ με/°C, and that of the FRP was $\alpha_{ft} = 32{\cdot}5$ με/°C (see Table 2). A temperature change of 30°C was assumed in the analysis which, if anything, may be a rather conservative estimate of a temperature change in practice.[24] The solution exposure and temperature conditions were taken to be independent and each effect was considered in isolation.

The concrete had a Poisson's ratio of $\nu_c = 0{\cdot}185$ with the creep and mix characteristics indicated in Table 3 and Figure 8. Concrete shrinkage effects were ignored. The concrete cover c was taken as 23 mm ($c/d \sim 5{\cdot}5$).[36] The transverse stiffness E_{22} (GPa) of the CFRP tendons was measured as 6·16 GPa.[37] As the Poisson's ratio of the FRP material was not determined in the current work, ν_{23} was taken to be 0·4 which is consistent with that reported elsewhere.[28]

Using the assumptions detailed above, the elastic concrete hoop stresses that can be expected at the tendon–concrete interface are plotted in Figure 10. The concrete hoop stresses adjusted for creep using the AAEM and the unadjusted stresses (no creep) are shown. The thermal strain was applied at $t = 0$, and sustained for the duration of the plot.

This figure indicates that in the early stage of exposure to solutions, the stress generated owing to the temperature change is the dominant effect. However, over time, swelling-induced stresses develop and eventually exceed those due to temperature. While concrete creep will help to reduce the hoop stresses generated, it is not necessarily sufficient to prevent the possibility of tensile cracking at the tendon–concrete interface. One caveat is that once cracking occurs, the uncracked elastic thick-walled analysis used in Figure 10 breaks down so, even for a high-strength concrete with say $\boldsymbol{f}_{ct} = 5$-6 MPa, the results at later times would be fictitious since cracking will have occurred. For comparison purposes, the predicted thermal stresses for an equivalent diameter steel rod with a Young's modulus of 210 GPa, a Poisson's ratio of 0·3 and CTE of 11 με/°C have also been included. It can be seen that the stresses generated are much smaller than either the FRP thermal or swelling results.

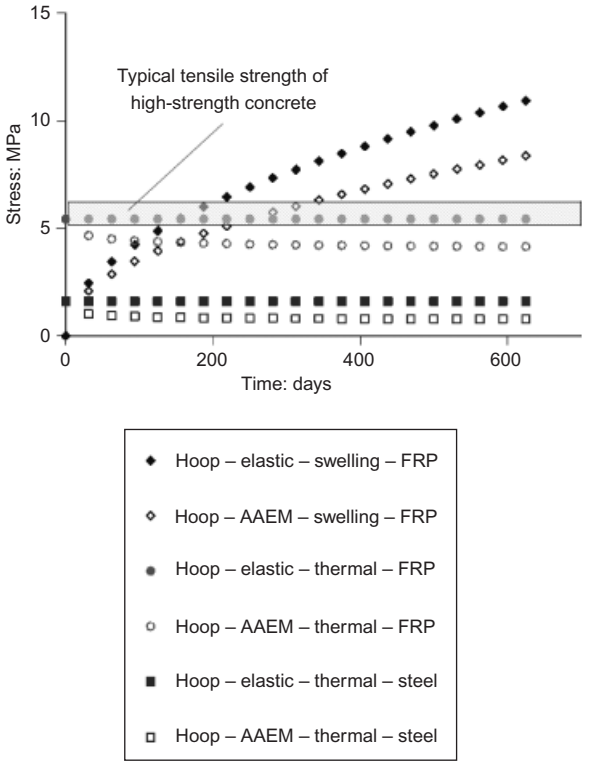

Figure 10. Effect of AAEM on hoop stresses in the concrete at the tendon interface

As a number of assumptions relating to the material properties and exposure conditions were used to plot Figure 10, a sensitivity study was also conducted. The baseline parameters were equivalent to those used in Figure 10 but no creep effects were included. For a given strain, each parameter was varied in turn using a multiplier ranging from 0·5 to 2 while all other parameters were held at their baseline values. The multiplier on the maximum hoop stress was calculated for each combination. The results are shown in Figure 11.

The hoop stress is directly proportional to ΔT, ΔM, β_{ft} and ($\alpha_{ft} - \alpha_c$) and this interaction can be seen in Figure 11. Variations in the assumed tendon material properties E_{22} and ν_{23} generally cause greater changes in hoop stress than the assumed concrete material properties E_c and ν_c. The sensitivity to the assumed tendon properties highlights the need to also understand how the tendon properties may change with time. Owing to the plasticisation of the matrix there could be changes in the FRP material properties due to exposure to

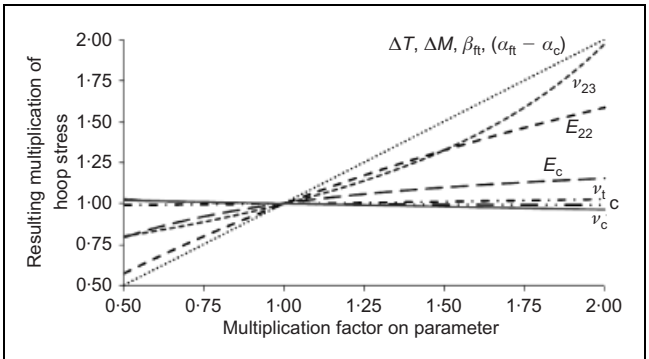

Figure 11. Sensitivity study of parameter input

solutions and/or temperature effects. This is an important area requiring further research.

Changes in the concrete cover do not have much of an influence on the maximum hoop stress generated. However, this should be treated with caution since the analysis in Figure 11 only considers elastic behaviour up to first cracking. The concrete cover will have much more of an influence when the partially cracked or plastic behaviour is assumed (see Figure 9) and it can be inferred that a thicker concrete cover will mitigate the possibility of concrete splitting. Similarly Figure 11 indicates the tendon radius has little effect on the hoop stress at the interface, although in practice this parameter will significantly effect the rate of uptake in the tendon, and hence the swelling occurring.

5. DISCUSSION

Based on the results in Figure 10, it would be expected that tendon swelling due to solution uptake could induce tensile stresses in the surrounding concrete, with potential implications that include concrete cracking and possible bond degradation. In addition, it appears that uptake-induced swelling of FRP tendons can be as significant a phenomenon as thermal effects, and it is curious that there has not been more research on the effects of FRP tendon swelling.

The measured swelling-induced strains from the FRP tendon uptake experiments were used in the analysis but it must be emphasised that these tendons had not yet reached saturation, and further swelling would occur. However, the swelling would not increase indefinitely and the increase in strain with time would be expected to slow significantly as the material approaches saturation so there will be a limit on the total strain expansion. Furthermore, the swelling measured here was attributed to continuous exposure to water or salt water. It will be important to consider in more detail the in-service exposure to solutions over the lifetime of a concrete structure and the associated presence of solutions at the tendon surface. In particular, the solution availability around the tendon is expected to be a key factor and this will depend on the exposure environment, for example wetting and drying conditions against full submersion, the concrete permeability, the presence of any cracks in the concrete and any solution retention at the tendon–concrete interface. A related study by the authors[37] has started to investigate possible profiles of solution concentration and initial results suggest that, when submerged, the tendon surface may experience conditions not dissimilar to those studied in these experiments.

It would seem plausible that, provided cracking does not occur, uptake-induced swelling of CFRP tendons may increase the contact pressure with the surrounding concrete, and therefore the bond. However, two studies have suggested that this is not the case. Davalos *et al.*[38] immersed concrete encased CFRP bars in water at either 20°C or 60°C for 90 days, and pullout tests showed bond strength to be 7·1% and 9·1% lower respectively than control specimens. The authors attributed the bond reduction to tendon degradation. Sen *et al.*[39] concluded that solution uptake effects were more significant than thermal effects in causing bond degradation and concrete cracking of CFRP prestressed structures. They exposed precracked pretensioned concrete beams with silica-coated CFRP tendons

to wet and dry cycles in a marine environment for 3 years. They found that solution uptake in the tendons reduced the bond capacity of the structures during the first 2 years of exposure, but tests at 3 years showed higher bond strength. They concluded that resin swelling was responsible for the initial bond degradation, but in the later stages of the test the solutions were able to diffuse to the inner regions of the tendon, explaining the recovery of bond strength. An alternative explanation based on the current findings would be that the initial bond strength loss is due to plasticisation of the silica-coated surface region of the tendon caused by initial solution ingress. At later times this effect is outweighed by swelling effects, which increase the tendon–concrete contact pressure, resulting in improved bond strength. However, in the longer term, if the pressure reaches a level that will cause cracking at the tendon–concrete interface, the bond could subsequently deteriorate.

The aforementioned papers highlight the difficulty in isolating the effect of uptake-induced swelling on bond while other aspects of tendon degradation may occur simultaneously and be contributing factors. The sand coating or other bond-enhancing features, often present on CFRP tendons, may complicate the effect that uptake-induced swelling has on the bond. Another complication is that the required timeframe to investigate solution uptake is potentially years. Although the uptake can be accelerated through the use of higher temperatures, this then makes it more difficult to separate temperature and solution uptake influences. A further consideration will be the possible consequences due to interactions between thermal and solution uptake effects. For example Adamson[20] found that saturating an epoxy in distilled water more than doubled the CTE of the material, due to increased bond disruption in the polymer. Further work is also required in order to correlate the effect of any longitudinal stress in the CFRP rod on the swelling behaviour and uptake-induced changes in the FRP material properties with time.

The significance of this research highlights the importance of considering uptake-induced swelling of CFRP tendons when designing reinforced or prestressed concrete structures. For a given concrete, FRP tendon and exposure conditions, design charts where the solution uptake with time is associated with a pressure generated at the tendon–concrete interface could be developed. These charts could be compared with appropriate theoretical predictions of the required cover to avoid splitting or excessive bond deterioration, for example along the lines of the failure criteria shown in Figure 9. Hence, in the same way that authors make recommendations for minimum concrete cover to allow for thermal effects, a similar approach should be adopted for uptake-induced swelling effects. Taking such steps in combination with using concrete of adequate tensile strength should be an effective means of avoiding spalling, although local micro-cracking and bond degradation may still occur. Swelling effects may also be minimised by taking steps to reduce the sensitivity of an FRP to solution uptake, for example by changing the resin chemistry.[4,6,40]

6. CONCLUSIONS

Dimensional changes may occur in FRPs due to thermal or solution uptake effects, and expansion or contraction transverse to the fibre direction can be expected. Experiments carried out on CFRP tendons have shown that the nature of the aqueous solution to which they are exposed makes little difference to the swelling observed and the relationship between the mass uptake and the increase in transverse strain was found to be linear. The uptake-induced swelling strains measured in the CFRP specimens studied have been shown potentially to exceed the anticipated thermal expansion strains that a structure may experience in service. However, the timeframe over which swelling may occur is much longer than temperature effects and so time-dependent changes in the surrounding concrete and the FRP reinforcement need to be taken into account. In the context of internal reinforcement for concrete, it is concluded that uptake-induced swelling could lead to concrete cracking and more research is required to investigate these effects in greater detail.

ACKNOWLEDGEMENTS

The authors would like to thank Dr Michael Sutcliffe from the University of Cambridge and Dr Giovanni Terrasi from EMPA for their help and support. They are also grateful for the practical assistance and guidance provided by David Miller, Alan Heaver and Roger Denston from the University of Cambridge. The research was also supported by SACAC, Switzerland through the provision of materials and technical assistance and the UK Engineering and Physical Sciences Research Council (EPSRC).

REFERENCES

1. McNeil I. *An Encyclopaedia of the History of Technology*. Taylor & Francis, Abingdon, 1990.
2. Strong A. B. *Plastics: Materials and Processing*. Prentice-Hall, Upper Saddle River, NJ, 2000.
3. Shen C.-H. and Springer G. S. Moisture absorption and desorption of composite materials. *Journal of Composite Materials*, 1976, **10**, No. 1, 2–20.
4. Adams R. D. and Singh M. M. The dynamic properties of fibre-reinforced polymers exposed to hot, wet conditions. *Composites Science and Technology*, 1996, No. 8, **56**, 977–997.
5. Tsai C.-L., Tsai Y.-S. and Chiang C.-H. The effects of hygric pressure, salt concentration and temperature on the hygric expansion of composite material. *Composites Science and Technology*, 2002, **62**, No. 6, 799–803.
6. Abot J. L., Yasmin A. and Daniel I. M. Hygroscopic behavior of woven fabric carbon: epoxy composites. *Journal of Reinforced Plastics and Composites*, 2005, **24**, No. 2, 195–207.
7. Cairns D. S. and Adams D. F. Moisture and thermal expansion properties of unidirectional composite materials and the epoxy matrix. In *Environmental Effects on Composite Materials* (Springer G. S. (ed.)). Technomic Publishing Company, Lancaster, PA, USA, 1984, pp. 300–316.
8. Collings T. A. and Stone D. E. W. Hygrothermal effects in CFRP laminates: strains induced by temperature and moisture. *Composites*, 1985, **16**, No. 4, 307–316.
9. Tsai C.-L., Wang C. H., Chang J.-J. and Yeih W. Tracking hygrothermal strains of carbon/epoxy composite under varying temperature and humidity. *Journal of Composite Materials*, 2008, **42**, No. 16, 1597–1618.
10. Wright W. W. The effect of diffusion of water into epoxy resins and their carbon-fibre reinforced composites. *Composites*, 1981, **12**, No. 3, 201–205.

11. Loh W. K., Crocombe A. D., Abdel Wahab M. M. and Ashcroft I. A. Modelling anomalous moisture uptake, swelling and thermal characteristics of a rubber toughened epoxy adhesive. *International Journal of Adhesion and Adhesives*, 2005, **25**, No. 1, 1–12.
12. Masmoudi R., Zaidi A. and Gerard P. Transverse thermal expansion of FRP bars embedded in concrete. *Journal of Composites for Construction*, 2005, **9**, No. 5, 377–387.
13. Kulkarni R. and Ochoa O. Transverse and longitudinal CTE measurements of carbon fibers and their impact on interfacial residual stresses in composites. *Journal of Composite Materials*, 2006, **40**, No. 8, 733–754.
14. Ishikawa T., Koyama K. and Kobayashi S. Thermal expansion coefficients of unidirectional composites. *Journal of Composite Materials*, 1978, **12**, No. 2, 153–168.
15. Tompkins S. S. Thermal expansion of selected graphite-reinforced polyimide-, epoxy- and glass-matrix composites. *International Journal of Thermophysics*, 1987, **8**, No. 1, 119–132.
16. American Concrete Institute. *ACI 440·3R-04: Guide Test Methods for Fiber-Reinforced Polymers (FRPs) for Reinforcing or Strengthening Concrete Structures*. ACI, Farmington Hills, Michigan, 2004.
17. Elbadry M. and Elzaroug O. Behaviour and design of structural concrete reinforces with CFRP rebars for temperature effects. *Proceedings of the 5th International Symposium on Fibre Reinforced Polymer for Reinforced Concrete Structures (FRPRCS-5)*, Cambridge, 2001, Volume 1, pp. 573–582.
18. Galati N., Nanni A., Dharani L., Focacci F. and Aiello M. A. Thermal effects on bond between FRP rebars and concrete. *Composites Part A: Applied Science and Manufacturing*, 2006, **37**, No. 8, 1223–1230.
19. Yoon K. J. and Kim J.-S. Prediction of thermal expansion properties of carbon/epoxy laminates for temperature variation. *Journal of Composite Materials*, 2000, **34**, No. 2, 90–100.
20. Adamson M. J. Thermal expansion and swelling of cured epoxy resin used in graphite/epoxy composite materials. *Journal of Materials Science*, 1980, **15**, No. 7, 1736–1745.
21. Yates B., McCalla B. A., Sargent J. P., Rogers K. F., Kingston-Lee D. M. and Phillips L. N. Thermal expansion of carbon fibre reinforced plastics—the influence of resin type. *Journal of Materials Science*, 1978, **13**, No. 10, 2217–2225.
22. Vogel H. and Svecova D. Thermal compatibility and bond strength of FRP reinforcement in prestressed concrete applications. *Journal of Composites for Construction*, 2007, **11**, No. 5, 459–468.
23. American Concrete Institute. *ACI 440.1R-03 Guide for the Design and Construction of Concrete Reinforced with FRP Bars*. ACI, Farmington Hills, Michigan, 2003.
24. Nanni A., Bakis C. E. and Boothby T. E. Test methods for FRP-concrete systems subjected to mechanical loads: state of the art review. *Journal of Reinforced Plastics and Composites*, 1995, **14**, No. 6, 524–558.
25. Elbadry M. M., Abdalla H. and Ghali A. Effects of temperature on the behaviour of fiber reinforced polymer reinforced concrete members: experimental studies. *Canadian Journal of Civil Engineering*, 2000, **27**, No. 5, 993–1004.
26. Abdalla H. Concrete cover requirements for FRP reinforced members in hot climates. *Composite Structures*, 2006, **73**, No. 1, 61–69.
27. Zaidi A. and Masmoudi R. Thermal effect on fiber reinforced polymer reinforced concrete slabs. *Canadian Journal of Civil Engineering*, 2008, **35**, No. 3, 312–320.
28. Aiello M. A., Focacci F. and Nanni A. Effects of thermal loads on concrete cover of fiber-reinforced polymer reinforced elements: theoretical and experimental analysis. *ACI Materials Journal*, 2001, **98**, No. 4, 332–339.
29. Lee M. C. and Peppas N. A. Water transport in epoxy-resins. *Progress in Polymer Science*, 1993, **18**, No. 5, 947–961.
30. Timoskeno S. P. and Goodier J. N. *Theory of Elasticity*, 3rd edn. McGraw-Hill, New York, 1988.
31. Neville A. M. *Properties of Concrete*, 4th edn. Addison Wesley, Harlow, 1997.
32. Liu L. and Weyers R. Modeling the time-to-corrosion cracking in chloride contaminated reinforced concrete structures. *ACI Materials Journal*, 1998, **95**, No. 6, November–December, 675–680.
33. Gilbert R. I. and Mickleborough N. C. *Design of Prestressed Concrete*. Unwin Hyman, London, 1990.
34. Tepfers R. Cracking of concrete cover along anchored deformed reinforcing bars. *Magazine of Concrete Research*, 1979, **31**, No. 106, 3–12.
35. Li C.-Q., Melchers R. E. and Zheng J.-J. Analytical model for corrosion-induced crack width in reinforced concrete structures. *ACI Structural Journal*, 2006, **103**, No. 4, July–August, 479–487.
36. Terrasi G. P. and Lees J. M. CFRP Prestressed Concrete Lighting Columns. In *Field Applications of FRP Reinforcement: Case Studies* (Rizkalla S. H. and A. Nanni A. (eds)). American Concrete Institute, Detroit, 2003, pp. 55–74.
37. Scott P. *Aspects of CFRP Prestressed Concrete Durability in the Marine Environment*. PhD thesis, University of Cambridge, UK. In preparation.
38. Davalos J. F., Chen Y. and Ray I. Effect of FRP bar degradation on interface bond with high strength concrete. *Cement and Concrete Composites*, 2008, **30**, No. 8, 722–730.
39. Sen R., Shahawy M., Rosas J. and Sukumar S. Durability of AFRP and CFRP pretensioned piles in a marine environment. *Proceedings of the 3rd International Symposium on Non-Metallic (FRP) Reinforcement for Concrete Structures (FRPRCS-3), Saporro,* 1997, Volume 2, 123–130.
40. Cohn D. and Marom G. Effect of the morphology on the hygroelastic behaviour of polyester and epoxy resins. *Polymer*, 1983, **24**, No. 2, 223–228.